Spin-to-Orbital Angular Momentum Conversion and Spin-Polarization Filtering in Electron Beams

Ebrahim Karimi,[1] Lorenzo Marrucci,[1,2,*] Vincenzo Grillo,[3,4] and Enrico Santamato[1]

[1]*Dipartimento di Scienze Fisiche, Università di Napoli "Federico II," Complesso Universitario di Monte S. Angelo, 80126 Napoli, Italy*
[2]*CNR-SPIN, Complesso Universitario di Monte S. Angelo, 80126 Napoli, Italy*
[3]*CNR-Istituto Nanoscienze, Centro S3, Via G Campi 213/a, I-41125 Modena, Italy*
[4]*CNR-IMEM, Parco delle Scienze 37a, I-43100 Parma, Italy*
(Received 3 March 2011; published 27 January 2012)

We propose the design of a space-variant Wien filter for electron beams that induces a spin half-turn and converts the corresponding spin angular momentum variation into orbital angular momentum of the beam itself by exploiting a geometrical phase arising in the spin manipulation. When applied to a spatially coherent input spin-polarized electron beam, such a device can generate an electron vortex beam, carrying orbital angular momentum. When applied to an unpolarized input beam, the proposed device, in combination with a suitable diffraction element, can act as a very effective spin-polarization filter. The same approach can also be applied to neutron or atom beams.

DOI: 10.1103/PhysRevLett.108.044801 PACS numbers: 41.85.Ct, 03.65.Vf, 03.75.−b

Phase vortices in electronic quantum states have been widely investigated in condensed matter, for example, in connection with superconductivity, the Hall effect, etc. Only very recently, however, free-space electron beams exhibiting controlled phase vortices have been experimentally generated in transmission electron microscope (TEM) systems, using either a spiral phase plate obtained from a stack of graphite thin films [1] or a "pitchfork" hologram manufactured by ion beam lithography [2,3]. In a cylindrical coordinate system r, ϕ, z, with the z axis along the beam axis, a vortex electron beam is described by a wave function having the general form $\psi(r,\phi,z,t) = u(r,z,t)\exp(i\ell\phi)$, where ℓ is a (nonzero) integer and u vanishes at $r=0$. As in the case of atomic orbitals, ℓ is the eigenvalue of the z-component orbital angular momentum (OAM) operator $\hat{L}_z = -i\partial_\phi$ (in units of the reduced Planck constant $\hbar$) and therefore an electron beam of this form carries $\ell\hbar$ of OAM per electron [4]. The recent experiments on electron vortex beams were inspired by the singular optics field, in which similar phase or holographic tools have been used in the last 20 years (see, e.g., [5] and references therein). In optics, a recently introduced alternative approach to the generation of vortex beams is based on the "conversion" of the angular momentum variation occurring in a spin-flip process into the orbital angular momentum of the light beam, when the latter is propagating through a suitable spatially variant birefringent plate [6,7]. In this Letter, we propose that a beam of electrons traveling in free space undergoes a similar "spin-to-orbital angular momentum conversion" (STOC) process in the presence of a suitable space-variant magnetic field. The same approach may work also for neutrons or any other particle endowed with a spin magnetic moment (e.g., atoms or ions). Of course, in the case of electrons, as for other charged particles, the magnetic field, besides acting on the spin, will also induce forces that must be compensated in order to avoid strong beam distortions or deflections. Such compensation may be obtained by a suitable electric field, and this leads us to conceiving the proposed apparatus essentially as a *space-variant Wien filter*. Such an apparatus can be exploited for generating vortex electron beams when a spin-polarized beam is used as input. Conversely, if a pure vortex beam is used as input, by means, e.g., of a holographic method, one can use the STOC process for filtering a single spin-polarized component of the input beam, as we will show further below.

Let us consider an electron beam propagating in vacuum along the z axis and crossing a region of space lying between $z=0$ and $z=L$ in which it is subject to electric and magnetic fields $\boldsymbol{E} = -\boldsymbol{\nabla}\Phi$ and $\boldsymbol{B} = \boldsymbol{\nabla}\times\boldsymbol{A}$, where Φ and $\boldsymbol{A}$ are the scalar and vector potentials, respectively. In the nonrelativistic approximation and neglecting all Coulomb self-interaction effects (small charge density limit), the electron beam quantum propagation and spin evolution are generally described by Pauli's equation

$$i\hbar\partial_t\tilde{\psi} = \left[\frac{1}{2m}(-i\hbar\boldsymbol{\nabla} - e\boldsymbol{A})^2 + e\Phi - \boldsymbol{B}\cdot\hat{\boldsymbol{\mu}}\right]\tilde{\psi}, \quad (1)$$

where $\tilde{\psi}$ is the spinorial two-component wave function of the electron beam, $e = -|e|$ and m are the electron charge and mass, ∂_t is the derivative with respect to the time variable t, and $\hat{\boldsymbol{\mu}} = -\frac{1}{2}g\mu_B\hat{\boldsymbol{\sigma}}$ is the electron magnetic moment, with $\mu_B = \hbar|e|/2m$ the Bohr's magneton, $g \simeq 2$ the electron g factor, and $\hat{\boldsymbol{\sigma}} = (\hat{\sigma}_x, \hat{\sigma}_y, \hat{\sigma}_z)$ the Pauli matrix vector.

As a first step, we consider the simpler case in which the electric and magnetic fields are taken to be uniform, lying in the transverse plane xy, and arranged as in standard Wien filters [8,9], i.e., perpendicular to each other and balanced so as to cancel the average Lorentz force, i.e., $E_0 = B_0 p_c/m$, where E_0 and B_0 are the electric and magnetic field moduli and p_c is the average beam momentum. The magnetic field $\boldsymbol{B}$ is also taken to form an arbitrary angle α with the axis x within the xy plane. For this case, we solved the full Pauli equation in the paraxial slow-varying-envelope approximation for an input beam having a Gaussian profile and an arbitrary uniform input spin state $|\psi\rangle_{\rm in} = a_1|\uparrow\rangle + a_2|\downarrow\rangle$, where $|\uparrow\rangle$ and $|\downarrow\rangle$ denote a state for which the spin is parallel or antiparallel to the z axis, respectively. The complete expression of the resulting spinorial wave function is given in the Supplemental Material (SM) [10], while here we summarize the main findings. The beam propagation behavior corresponds to the well-known astigmatic lensing in the plane perpendicular to the magnetic field. More precisely, the beam undergoes periodic width oscillations, with a spatial period $\Lambda_2 = \pi R_c$, where $R_c = p_c/(|e|B_0)$ is the cyclotron radius. This lensing phenomenon is also predicted by a classical ray theory, when properly taking into account the effect of the input fringe fields [10]. The output spin state is instead given by the following general expression (Eq. 4 in the SM [10])

$$|\psi\rangle_{\rm out} = a_1[\cos(\delta/2)|\uparrow\rangle + \sin(\delta/2)ie^{i\alpha}|\downarrow\rangle] + a_2[\cos(\delta/2)|\downarrow\rangle + \sin(\delta/2)ie^{-i\alpha}|\uparrow\rangle], \quad (2)$$

where $\delta = 4\pi L/\Lambda_1$ and $\Lambda_1 = 4\pi R_c/g \simeq 2\Lambda_2$. This spinorial evolution corresponds to the classical Larmor precession of the spin with spatial period $\Lambda_1/2$, δ being the total precession angle. However, in addition to the spin precession, Eq. (2) predicts the occurrence of wave function phase shifts. In particular, for a $|\uparrow\rangle$ or $|\downarrow\rangle$ input state and a total spin precession of exactly half a turn, i.e., $\delta = \pi$ or $L = \Lambda_1/4$, the wave function acquires a phase shift given by $\pm\alpha + \pi/2$, where α is the magnetic field orientation angle mentioned above and the $\pm$sign is fixed by the input spin orientation ($+$ for $|\uparrow\rangle$ and $-$ for $|\downarrow\rangle$). These phase shifts can be interpreted as a special case of *geometric Berry phases* arising from the spin manipulation [11].

Let us now move on to the case of a spatially variant magnetic field. We consider multipolar transverse field geometries with cylindrical symmetry, described by the following expression for the magnetic field (with the vector given in Cartesian components): $\boldsymbol{B}(r, \phi, z) = B_0(r)(\cos\alpha(\phi), \sin\alpha(\phi), 0)$, where the angle α is now the following function of the azimuthal angle:

$$\alpha(r, \phi, z) = q\phi + \beta, \quad (3)$$

where q is an integer and β a constant. Clearly, such a field pattern must have a singularity of topological charge q at $r = 0$. In particular, by imposing the vanishing of the field divergence, we find that the radial factor $B_0(r) \sim r^{-q}$, i.e., the field vanishes on the axis for $q < 0$, while it diverges for $q > 0$. In the latter case, there must be a field source on the axis. We call a balanced Wien filter whose magnetic field distribution in the beam transverse plane obeys Eq. (3) a "q filter." The electric field will be taken to have an identical pattern, except for a local $\pi/2$ rotation, so as to balance the Lorentz force. Some examples of such q-filter field distributions are shown in Fig. 1. We are particularly interested in the negative q geometries, which do not require us to have a field source at $r = 0$. For example, the $q = -1$ case corresponds to the standard quadrupole geometry of electron optics, while $q = -2$ corresponds to the hexapole one. Wien filters with such geometries have already been developed in the past for the purpose of correcting chromatic aberrations [12,13]. Moreover, inhomogeneous Wien filters, including several multipolar terms, have also been considered for the purpose of spin manipulation, with the added advantage of obtaining a stigmatic lensing behavior [14]. A possible design of the $q = -1$ filter with quadrupolar geometry is shown in Fig. 2. In such nonuniform field geometry, we cannot solve analytically the full Pauli equation. However, the beam propagation is already well-described by classical dynamics and can be derived either analytically, using a power expansion in r [14], or by numerical ray tracing. In the former case, we find that to first order the q filter for $q \neq 0$ is already stigmatic, i.e., it preserves the beam circular symmetry. Only second-order corrections introduce aberration effects [14]. This behavior is confirmed by our numerical ray-tracing simulations (see the SM for details [10]), which show relatively weak higher-order aberrations (see Fig. 2). It should be noted that these simulations have been performed for realistic values of the electric and magnetic fields, as required to obtain a spin precession of half a turn across a propagation distance of 50 cm at a beam radius of 100 μm. These calculations are expected to reproduce very well the electron density behavior (and spin precession) as would be obtained from Pauli's equation. However, Pauli's equation predicts an additional purely quantum phenomenon, namely, the geometric phase already discussed above. In a semiclassical approximation, the geometric phase will still be given by $\pm\alpha + \pi/2$, where α is, however, now position-dependent and given by Eq. (3). More specifically, neglecting the aberrations,

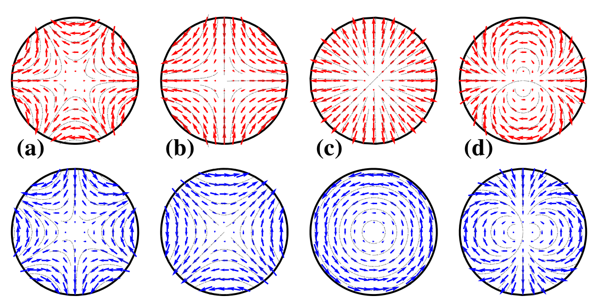

FIG. 1 (color online). Electric (upper panels) and magnetic (lower panels) field q-filter geometries for different topological charges: (a) $q = -2$, (b) $q = -1$, (c) $q = 1$, and (d) $q = +2$; in all cases, $\beta = \pi/2$.

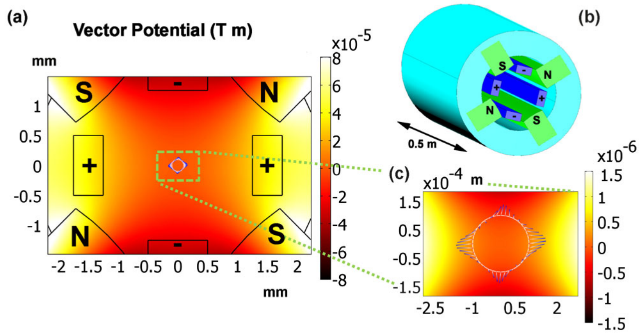

FIG. 2 (color online). Electrodes and magnetic pole geometry of a q filter with $q = -1$ (quadrupole), seen in (a) cross sectional and in (b) three-dimensional rendering. The filter length is set to 50 cm. In (a), the calculated vector potential A_z (in false colors), which is also roughly proportional to the electric potential, and the projection on the xy plane of the simulated electron ray trajectories for 100 keV energy are also shown (see the SM for details about the simulations [10]) for a ring-shaped input beam with radius $r = 100\ \mu\text{m}$ (ray color grows darker for increasing z). In (c), a zoomed-in view of the central region is shown. The magnetic field at r needed to obtain the tuning condition $\delta = \pi$ is 3.5 mT, with a corresponding electric field of 575 kV/m. These are obtained with an electrode potential difference of ≈ 9 kV and a magnetization of 135 A/mm. The fields need to be set to the design values with a precision of 1 part in 10^4.

each possible electron trajectory within a beam is straight and parallel to the z axis. Therefore, the electrons traveling in a given trajectory will experience a constant magnetic field of modulus $B_0(r)$ and orientation $\alpha(\phi)$. The set of all electrons traveling at a given radius r will then undergo a uniform spin precession by angle $\delta(r)$ and, if $\delta(r) = \pi$ (i.e., for a spin half-turn rotation), they will also acquire a space-variant geometric phase given by $\pm\alpha(\phi) + \pi/2 = \pm q\phi \pm \beta + \pi/2$, with the $\pm$ sign determined by the input spin orientation. In other words, the outgoing wave function acquires a phase factor $\exp(i\ell\phi)$, with $\ell = \pm q$, corresponding to a vortex beam with OAM $\pm q\hbar$. In a quantum mechanical notation, spin-polarized input electrons with given initial OAM ℓ passing through a q filter undergo the following transformations:

$$\begin{aligned} |\uparrow, \ell\rangle &\rightarrow \cos(\delta/2)|\uparrow, \ell\rangle + ie^{i\beta}\sin(\delta/2)|\downarrow, \ell + q\rangle, \\ |\downarrow, \ell\rangle &\rightarrow \cos(\delta/2)|\downarrow, \ell\rangle + ie^{-i\beta}\sin(\delta/2)|\uparrow, \ell - q\rangle, \end{aligned} \tag{4}$$

where the ket indices now specify both the spin state (arrows) and the OAM eigenvalue.

Equations (4) show that, in passing through the q filter, a fraction $f = \sin^2(\delta/2)$ of the electrons in the beam will flip their spin and acquire an OAM $\pm q\hbar$, while the remaining fraction $1 - f = \cos^2(\delta/2)$ will pass through the filter with no change. When $L = \Lambda_1/4$, then $\delta = \pi$ and all electrons are spin-flipped and acquire the corresponding OAM. In the specific case of $q = 1$, the spin angular momentum variation for the electrons undergoing the spin inversion is exactly balanced by the OAM variation, so that the total electron angular momentum remains unchanged in crossing the filter. This is the pure STOC process mentioned in the Introduction and it occurs for $q = 1$ because this geometry is rotationally invariant and therefore no angular momentum can be exchanged with the field sources in the filter. In the $q \neq 1$ case, the input spin still controls the sign of the OAM variation but the total beam angular momentum is not conserved and some angular momentum is exchanged with the field sources. We note that this OAM variation can also be explained as the effect of the spin-related magnetic-dipole force acting on the electrons within the magnetic field gradients, as more fully discussed in the SM [10].

The "tuning" condition $L = \Lambda_1/4$ or $\delta = \pi$ can be achieved in principle for a given radius r by adjusting the strength of the magnetic and electric fields or the device length L. Since the precession angle δ is r-dependent, however, this tuning condition can be applied to the entire beam only if it is shaped as a ring, i.e., with all electron density peaked at a given radius r. Vortex beams with OAM $\ell \neq 0$ typically have a doughnut shape, so they approximate a ring fairly well. On the other hand, a Gaussian input beam (with $\ell = 0$) cannot be fully transformed, as $\delta = 0$ at $r = 0$, where the beam has the maximum density. In such cases, only a fraction f of the electrons would be converted.

So far, we have assumed a spin-polarized input beam. However, high brightness (i.e., spatially coherent) spin-polarized electron beams, suitable for high-resolution TEM applications, are not so easily available. State-of-the-art spin-polarized sources may achieve a brightness of $10^7\ \text{A}\,\text{cm}^{-2}\,\text{sr}^{-1}$ and a polarization purity of up to 90% [15] (and the source decays with time due to laser-induced damage). It is interesting then to analyze the effect of the q filter on an initially unpolarized electron beam, having arbitrary initial OAM ℓ. Such an input can be simply viewed as a statistical mixture in which 50% of the electrons are in the state $|\uparrow, \ell\rangle$ and 50% in the state $|\downarrow, \ell\rangle$. After passing through a tuned q filter, the beam becomes a 50-50 mixture of states $|\downarrow, \ell + q\rangle$ and $|\uparrow, \ell - q\rangle$, for which spin and OAM are correlated (if the q filter is not tuned, the fraction of converted electrons decreases to $f/2$ in each spin-orbit state and there will be a residual $1 - f$ fraction of electrons in states $|\uparrow, \ell\rangle$ and $|\downarrow, \ell\rangle$). As we discuss now, this spin-OAM correlation can be exploited for making an effective electron beam spin-polarization filter. Such a filter requires four basic elements in sequence (as shown in Fig. 2 of the SM [10]): (i) an OAM manipulation device, such as a fork hologram [2,3], to set $\ell \neq 0$; (ii) a q filter with $q = \ell$, generating a mixture of electrons in states $|\downarrow, 2\ell\rangle$ and $|\uparrow, 0\rangle$; (iii) a free propagation (or imaging) stage that allows these two states to develop different radial profiles by diffraction because of their different OAM values; and

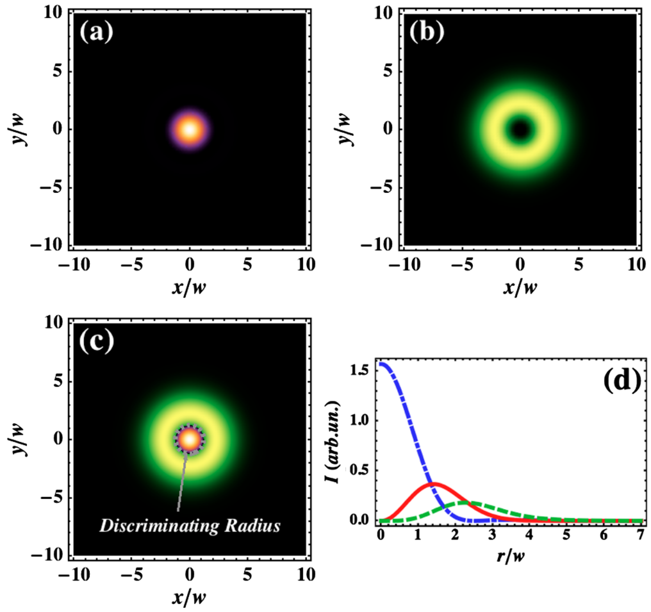

FIG. 3 (color online). Electron beam profiles in the far field of the q filter for (a) the $\ell = 0$ component and (b) the $\ell = 2$ component and (c) a possible discriminating iris radius $r = w$ to be used to separate them in order to make a spin-polarization filter. (d) shows the intensity profiles of the same components ($\ell = 0$, dot-dashed blue line; $\ell = 2$, dashed green line) and of the possible residual $\ell = 1$ component for an untuned q filter (solid red line). w is the Gaussian beam waist radius in the far-field plane. A realistic value for the iris radius is of the order of several tens of microns (obtained by setting the aperture some distance after the focal plane of the second condensor).

(iv) a circular aperture for finally separating the two states. In particular, in stage (iii), state $|\downarrow, 2\ell\rangle$ will acquire a radial doughnut distribution, as in Laguerre-Gaussian modes with OAM 2ℓ, which vanishes close to the beam axis as $r^{2\ell}$, while state $|\uparrow, 0\rangle$ will become approximately Gaussian, with maximum intensity at the beam axis, as shown in Figs. 3(a) and 3(b). Therefore, a suitable iris [Fig. 3(c)] will select preferentially the electrons in the fully polarized state $|\uparrow, 0\rangle$. An optical OAM sorter exploiting a similar approach has been demonstrated recently [16]. A specific calculation for the case of $|q| = |\ell| = 1$ and an iris radius equal to the beam waist w in the "far field" yield a transmission efficiency of our device of 55.5% (not including the losses arising in the OAM manipulation device) and a polarization degree $(I_\uparrow - I_\downarrow)/(I_\uparrow + I_\downarrow)$, where $I_{\uparrow,\downarrow}$ are the two spin-polarized currents, of ~97.5%. Higher degrees of polarization can be obtained at the expense of the efficiency by reducing the iris diameter or by employing higher q values (or vice versa). It is worth noting that this apparatus works also with a partially tuned q filter, as in this case the unmodified electron beam component is left in the initial OAM state $\ell = q$ and therefore is also cut away by the iris. An untuned q filter will, however, have an efficiency reduced by the factor $f = \sin^2(\delta/2)$. The aberrations introduced by the q filter, even if left uncorrected, might also affect its efficiency but not its main working principle, as this is based on the vortex effect, which is protected by topological stability. Finally, the possible spin depolarization effect of fringe fields can be neglected if the length-to-gap ratio of the filter is large enough [10,14].

We note that the spin-filter application discussed above is a new counterexample of the old statement by Bohr that free electrons cannot be spin-polarized by exploiting magnetic fields, due to quantum uncertainty effects [17–19]. The reason why we can overcome Bohr's arguments is essentially that we do not use the magnetic forces directly to obtain the separation but take advantage of quantum diffraction itself, as also proposed recently in Ref. [20] (see the SM for a fuller discussion [10]).

In conclusion, we believe that the q-filter device described in this Letter can be manufactured relatively simply for applications in standard electron beam sources such as those used in TEMs or other kinds of electron microscopes. In combination with current field-effect unpolarized electron sources, such a filter might provide a spin-polarized source with a brightness $\sim 10^9\ \mathrm{A\,cm^{-2}\,sr^{-1}}$, about 2 orders of magnitude higher than the current state of the art. This result, if it will be proved practical enough, may open the way to a spin-sensitive atomic-scale TEM, e.g., one suitable for investigating complex magnetic order in matter or for spintronic applications.

We acknowledge the support of the FET-Open Program within the 7th Framework Programme of the European Commission under Grant No. 255914, Phorbitech.

*marrucci@na.infn.it

[1] M. Uchida and A. Tonomura, Nature (London) **464**, 737 (2010).
[2] J. Verbeeck, H. Tian, and P. Schattschneider, Nature (London) **467**, 301 (2010).
[3] B. J. McMorran *et al.*, Science **331**, 192 (2011).
[4] K. Y. Bliokh, Y. P. Bliokh, S. Savel'ev, and F. Nori, Phys. Rev. Lett. **99**, 190404 (2007).
[5] S. Franke-Arnold, L. Allen, and M. J. Padgett, Laser Photon. Rev. **2**, 299 (2008).
[6] L. Marrucci, C. Manzo, and D. Paparo, Phys. Rev. Lett. **96**, 163905 (2006).
[7] L. Marrucci *et al.*, J. Opt. **13**, 064001 (2011).
[8] V. Tioukine and K. Aulenbacher, Nucl. Instrum. Methods Phys. Res., Sect. A **568**, 537 (2006).
[9] J. Grames *et al.*, *Proceedings of the 2011 Particle Accelerator Conference, New York, NY, USA* (to be published).
[10] See Supplemental Material at http://link.aps.org/supplemental/10.1103/PhysRevLett.108.044801 for further details.
[11] *Geometric Phases in Physics*, edited by A. Shapere and F. Wilczek (World Scientific, Singapore, 1988).
[12] H. Rose, Optik **32**, 144 (1970).

[13] J. Zach and M. Haider, Nucl. Instrum. Methods Phys. Res., Sect. A **363**, 316 (1995).
[14] M. R. Scheinfein, Optik **82**, 99 (1989).
[15] N. Yamamoto *et al.*, J. Phys. Conf. Ser. **298**, 012017 (2011).
[16] E. Karimi *et al.*, Appl. Phys. Lett. **94**, 231124 (2009).
[17] O. Darrigol, Historical studies in the physical sciences **15**, 39 (1984).
[18] H. Batelaan, T. J. Gay, and J. J. Schwendiman, Phys. Rev. Lett. **79**, 4517 (1997).
[19] G. A. Gallup, H. Batelaan, and T. J. Gay, Phys. Rev. Lett. **86**, 4508 (2001).
[20] S. McGregor *et al.*, New J. Phys. **13**, 065018 (2011).